

QUT Digital Repository:
<http://eprints.qut.edu.au/>



Ho, Tin Kin and Liu, S. Y. and Lee, K. Y. and Ho, Y. T. and Ho, K. H. and McCusker, A. and Kam, J. and Tam, H. Y. and Ho, S. L. (2009) *An investigation of rail condition monitoring by fibre Bragg grating sensors*. Hong Kong Institution of Engineers, Transactions, 16(2). pp. 9-15.

© Copyright 2009 Hong Kong Institution of Engineers

An Investigation of Rail Condition Monitoring by Fibre Bragg Grating Sensors

T.K. Ho^a, S.Y. Liu^a, K.Y. Lee^b, Y.T. Ho^c, K.H. Ho^c, H.Y. Tam^a and S.L. Ho^a

^a Department of Electrical Engineering, Hong Kong Polytechnic University

^b MTR Corporation Limited, Hong Kong

^c Department of Engineering, Hong Kong Institute of Vocational Education (Tsing Yi), Hong Kong

Abstract: Condition monitoring on rails and train wheels is vitally important to the railway asset management and the rail-wheel interactions provide the crucial information of the health state of both rails and wheels. Continuous and remote monitoring is always a preference for operators. With a new generation of strain sensing devices in Fibre Bragg Grating (FBG) sensors, this study explores the possibility of continuous monitoring of the health state of the rails; and investigates the required signal processing techniques and their limitations.

Introduction

Rails and trains are the two essential physical assets in railway operations. The frequent interactions between rails and train wheels inevitably lead to gradual deterioration on both parties. While wheel defects can be detected and repaired in the depot during regular maintenance, rail defect detection is only carried out on site and usually outside service hours, either manually or through advanced technologies.

Ultrasonic detection has recently become a popular means of rail condition monitoring [1, 2]. The equipment is mounted on a self-powered car and hand inspection was made along the line. This approach has been proven to be effective in identifying defects, but it does not discriminate the causes of defects, nor does it predict potential defects. The equipment is operated manually and the inspections are only conducted when the railway line is not in service.

Strain gauges, magnetic coils and Hall sensors are among other commonly adopted rail defect detectors. The data is collected along the track and passed to a central control room via telephone link or other communication means. This setup enables automatic and remote monitoring but the bandwidth of the communication channel limits the number of detection devices. The information received may not be able to support sophisticated signal processing

analysis. Further, electromagnetic interference in an electrified railway always imposes technical difficulties on the reliability of the data collected.

In other words, the current technologies of rail defect detection are barely adequate. For heavily utilised railway systems as in Hong Kong, it is therefore desirable for the operator to be able to conduct continuous on-line monitoring on the rail condition with full automation and substantial accuracy and reliability.

The dynamics of rail-wheel interactions, occurring whenever a train is running on the rail, is a good indication of the states of rails and wheels [3, 4]. As a result, it is possible to deduce the health condition of the rail (or at least detect any deviation from the health state) if reliable on-line collection of data on rail-wheel interactions is available and appropriate signal processing techniques are employed to analyse the data.

An optical fibre sensor system with Fibre Bragg Grating (FBG) technology has been installed on the East Rail line of the MTR system in Hong Kong, initially for the purpose of train detection [5]. The sensors are installed along the track and data on rail-wheel interactions are collected in real-time through an exclusive and reliable optical communication link. This study attempts to extract the signatures of the signals collected by FBG sensors, which reflect the health state of the rail; and to identify the difficulties and limitations of turning this continuous remote sensing system into practical implementation. Railway operation is a technologically demanding environment for applications of new technologies and this work explores the benefits of the advanced optical fibre sensing technology in railway condition monitoring.

Rail-wheel Interactions

The dynamics of rail-wheel interactions is a complicated process. It is known to be a stable closed system [3] in which the oscillations of the rail lead to fluctuating contact forces which then excite the rail. The instantaneous strain on the rail-wheel contact point records the characteristics of the dynamics and it in turn provides an indication of the health condition of both rails and wheels. Such characteristics (or signatures) in the rail-wheel interaction signals come from two primary attributing sources, the rail and its support; and the train running upon the rail.

The rail is supported by sleepers which are dynamic vibration absorbers and hence vibrations of certain frequencies are expected. The rail profile, track layout in the vicinity (e.g. adjacent line or junction nearby); soil properties; ballast condition; or even presence of trackside equipment may also determine the infrastructure natural frequency. On the other hand, as the train exerts the excitation force to the rail, its weight and speed, which vary during operation, also contribute to the signatures of the rail-wheel interaction signals. Further, external factors, such as weather, materials tear-and-wear, and driving patterns, also have a part to play. Hence, the signal signatures are likely to be unique at the individual points of measurement.

Because of the complexity of the rail-wheel interaction dynamics and the numerous external factors, there are no standard techniques for thorough analysis. Simulation is one of the conceivable means in which the accuracy of models and the levels of details of the results are the key concerns. Strain gauges, among other traditional sensors, are the possible sensing devices to measure the rail-wheel interaction dynamics, but they are all susceptible to electromagnetic interference in electrified railway systems.

This study is to extract the signatures from the collected signals at designated FBG sensors and establish if repeated signatures are found under the same wheel states and operation conditions. Real-life data are collected from the East Rail line for nearly four months and the rail condition at the measuring points has been verified to be healthy. Signals of the same wheel of the trains running on the same measuring points at roughly the same time of the day have been grouped together for analysis and comparisons.

Optical Fibre Sensing System

Fibre Bragg Grating (FBG) sensors are narrow-band optical reflectors that are induced inside telecommunication fibres using ultra-violet light to form permanent periodic refractive index change in the fibre core. FBG sensors reflect light with wavelength that satisfies the Bragg's condition [6]. Strain induced to FBG sensor causes a shift in its Bragg wavelength. As a result, the sensors can be employed as highly sensitive strain gauges while the shift in wavelength is detected through a FBG interrogator. As one FBG sensor only occupies a spectral width of 1 nm for effective strain measurement, an interrogator with light source of 100 nm is able to cope with 100 sensors simultaneously over a single strand of optical fibre. The key advantage of FBG sensors is that the measured strains are represented by the variations in wavelength, which is an

absolute parameter and hence not subject to signal attenuation over distance. Immunity to electromagnetic interference is a genuine bonus of FBG sensors, particularly for applications in an EM-hostile environment of electrified railways.

The set-up of the optical fibre sensing system is illustrated in Figure 1. The FBG sensors are fixed at the foot of the rail web while a number of sensors are induced on the same optical fibre. A light source of specified bandwidth in the interrogator is fed into the optical fibre and the wavelengths of the reflected light are recorded by the interrogator. The data on wavelength variations are then transferred to a computer for processing and analysis. The interrogator is able to serve a number of FBG sensors on the same optical fibre and there is no limitation on the distance between the sensors and the interrogator, which is particularly suitable for remote sensing.

FBG sensors have found numerous successful applications in condition monitoring of infrastructures [7] and their applications in railways have shown promising results [8, 9]. In a study on train detection, a number of FBG sensors are installed along the rail on an existing line and each rail-wheel interaction is measured as a change in strain on the rail [5]. Hence, the passage of each wheel is detected and registered accordingly and train detection is realised by counting the wheels in and out of a section, in the similar approach as axle counters. The results from on-site measurements show very consistent performance and they are comparable with those from the existing train detection systems.

Preliminary Works

Data collected from a FBG sensor installed close to the Fo Tan Station of the East Rail Line at the MTR system in Hong Kong have been used in a preliminary study [10]. Signals of the rail-wheel interactions of the same bogie (i.e. two wheels) of the train running at the same time of the day over a few months (103 days) are extracted. The speed of the train running over the measurement point is also deduced from the data. The sampling frequency at each sensor is 1 kHz. An example of the collected rail-wheel interaction signal is given in Figure 2. The two peaks correspond to the two wheels of the bogie and the change of wavelength is within 0.2nm (i.e. between 1561.84nm and 1562.04nm) and the train speed is estimated by the time difference of the two peaks and the known distance between the two wheels. As each FBG is inscribed with a different reflected wavelength to cover the bandwidth of the light source, the absolute

value of the wavelength range of each FBG sensor is different. It is, however, the variations of wavelength which are of interest in this study as they represent the changes of strain at the rail contact point. The subsequent analysis hence focuses on the changes of reflected wavelength due to the rail-wheel interactions.

It is important to note that the field measurement data exhibit very high signal-to-noise ratio even without any signal processing. For the signal in Figure 2, as the FBG interrogator is also located at the Fo Tan Station, the distance between the physical sensor and the interrogator is only 30m. Another sensor is installed at the Tsim Sha Tsui Tunnel which is 13.6 km from the interrogator. The signals collected, as shown in Figure 3, through the optical communication link along the East Rail line enables very much identical signal-to-noise ratio and thus signal quality despite the distance.

The contents of frequency spectrum of the signals are investigated in the preliminary study. As the signals are non-periodic, Wavelet Transforms are employed to extract the frequency spectrum [11]. A set of decomposed signals at distinct frequency bands, which contains independent dynamic information, is provided by Wavelet Transforms. Comparisons are then conducted among the signals at the same decomposed frequency bands. Figure 4 illustrates an example of the decomposed signals over the successive frequency bands. It is literally a spectral breakdown of the original signal over the successive frequency bands and the details of the contents in the frequency bands are given as time waveforms. The lowest decomposed frequency band attained here covers the frequency range of 2.6-5.2 Hz. It is possible to go below this frequency range, but further decomposition may not be able to offer more useful information as the number of samples shrinks while de-sampling continues with each decomposition level through Wavelet Transforms.

In order to determine if the content in each frequency band of decomposed signal contains useful information, Auto-correlation has been conducted on the time waveforms of individual frequency bands. As revealed in Figure 5, the first four levels (i.e. high-frequency components) mainly consist of noise because of the single distinctive strong burst in the middle; and the signal signature, if any, should be contained in the subsequent levels (i.e. low-frequency components). However, while the Wavelet Transforms only allow signal decomposition to go down to the frequency band of 2.6-5.2 Hz, certain signal characteristics below this frequency band, if ever exists, are not made available and the signal signature may not have been entirely extracted.

The signal decompositions on data collected daily during the measurement period are then compared by simple visual inspection, particularly in frequency bands lower than 40 Hz (i.e. levels 5-7). It is apparent that the signal pattern in each decomposed level is similar, suggesting there is a substantial extent of repeatability. However, it is not possible to quantify the similarities by visual comparison. For the purpose of rail defect detection, an objective threshold of similarity is essential to discriminate between health rail and otherwise. On the other hand, this threshold should be robust enough to accommodate the differences in signals due to variations in train operation conditions, such as train weight and speed.

Signal Analysis

In order to establish if the signal patterns at decomposed frequency bands are repeatable under the same operation conditions, an objective comparison with a quantitative means is required. Correlation is a commonly adopted signal processing technique to measure the similarity between two signals [12]. It is useful for comparing signals with a pre-defined reference and attaining the closeness between them. Prior to applying Correlation, the signals have to be pre-processed to eliminate or minimise the effects of external factors on signals signature due to rail-wheel interaction.

During a rail-wheel interaction, the strain on the rail is directly related to the weight of the train. As a result, the magnitude of the signals collected from the FBG sensors may vary with the weight of train but it is not related to the health state of the rail. To eliminate the effect of varying magnitudes, the decomposed signal at each frequency band is then normalised in magnitude and its average value is taken away (the signal may retain a dc value because of the interactions with the mother wavelet during Wavelet Transforms). Before the comparison among the signals, the characteristics of signals are analysed through Auto-correlation. The peak values of Auto-correlation on signals of the lower 3 decomposed frequency bands (i.e. levels 5-7) on data from one sensor over the measurement period of 103 days are summarised in Table 1. The lowest decomposed frequency band (i.e. level 8) is not included as it contains too few data points for reasonable analysis.

From Table 1, it is clear that the signals still contain substantial variations from the viewpoint of a clear-cut numerical indication despite having similar patterns at different decomposed

frequency bands. The implication is that it is difficult to define a reference for comparison in determining the rail condition.

Upon further inspection of the data, even though the signals are from the same wheels running over the same measurement point at the same time of the day, the train speed is not necessarily the same. During the measurement time, the instantaneous train speed is found to vary between 9.698 kph and 15.126 kph. As the train speed increases, the duration of the signal pulses collected, as illustrated in Figure 1, becomes shorter and the signal is literally ‘compressed’ on the time scale. Hence, the Auto-correlation on the decomposed frequency bands inevitably produces different peak values.

To further illustrate the effect of train speed even within the narrow range between 9.698 kph and 15.126 kph, the peak values of Cross-correlations between the signals at the decomposed frequency bands, with the signals of the highest, median and lowest train speeds of this speed range as references respectively, are listed in Tables 2. For easier comparisons, normalisation of area enclosed by the signals is also carried out in order to standardise the power content of the signals (i.e. the peak value of Auto-correlation on each signal is standardised to an arbitrary value of x_{ref}). When the signals are completely repeatable (i.e. identical signals), the peak value of cross-correlation is x_{ref} . The less the similarities between two signals are, the lower the value (or farther away from x_{ref}) is. For the results shown in Table 2, x_{ref} is taken as 4.

There are significant variations in the peak correlation values with even a small change of train speed, which reiterates the difficulty of identifying a suitable numerical reference for signal-similarity comparisons. As expected, when the signal with the median speed is employed as the reference, better similarity is attained on average.

The analysis is then extended to 12 speed groups with train speed spanning over a wider range, and particularly higher train speed. Data is collected from the wheels of an accelerating train running upon the same sensor at the same location and hence the train speed on successive wheels is increasing gradually. As a result, the average speeds of the 12 speed groups go from 12.97 kph to 64.73 kph (i.e. each speed group covers 4-5 kph) are recorded. The average peak values of Cross-correlation in the lower 3 decomposed frequency bands (i.e. levels 5-7) over the measurement period of 103 days are given in Figures 6, 7 and 8 respectively. Again, the signals

with the highest, median and lowest train speeds within each speed group are taken as references with Cross-correlation.

The results indicate reasonable similarities among the signals over the 3 frequency bands but there are still certain variations with train speed. With the signals of the median speeds in the speed group as reference, the best similarities are obtained. When train speed becomes higher, the number of sampled data over the duration of the rail-wheel interactions decreases, so does the number of data points available to the lower frequency band (i.e. level 7). The signal pattern at decomposition level 7 may be distorted due to insufficient data and hence the comparisons do not necessarily reflect the extent of similarities, which explains the irregular fluctuations in Figure 8, particularly toward the higher-speed end. Therefore, it calls for a higher sampling rate for the sensors in order to cover the rail-wheel interactions under high train-speed operations. However, the sampling rate of this sensing system cannot be raised without significant implication on cost. The requirements for higher sampling rate will be discussed in the subsequent section.

Train Speed Effect

Train speed inevitably imposes a substantial impact on the signal signature on FBG sensors but the corresponding change in the signal signature does not reflect the actual health state of the rail. As a train usually runs on a wide range of speeds, rail condition detection through the signals on rail-wheel interactions have to eliminate the train speed effect before the signals are to be put through any signal processing or analysis for comparison.

A simple way to tackle this problem is to have a number of speed groups and the signal from a particular train speed is only compared with the reference of the relevant speed group. However, as each speed group only covers a small range of speed, there will be quite a number of speed groups in which the references are to be determined.

An alternative is to adjust the time scale according to the difference in train speed. In other words, only the shape or pattern of the signals is compared while the time scale is 'normalised' to put the signals on the same time-span. It should be noted that the frequency content of the signal would have been distorted if the time scale was adjusted. This approach can only be applied to decomposed signals after the Wavelet Transforms and it is to pursue detection of

similar pattern between signals. Adjustment of time-scale means addition or deletion of data points in the signals. When the decomposition of signal with Wavelet Transforms goes further with even lower frequency range, the number of data points in the decomposed signal reduces substantially because of continuous de-sampling. It becomes difficult to add in or dump data points without unnecessarily jeopardising the overall integrity of the signals. The issue of higher sampling rate of the sensor surfaces again.

Further Works

From the results so far, the signals in decomposed frequency bands show good consistency in general, which implies certain extent of repeatability of signals collected under the same or very similar operation conditions. However, there are still practical difficulties on establishing quantitative indications in similarity. For example, train speed is one of the main contributors towards variations of signals. Signal comparisons through signal processing techniques are not yet conclusive, particularly for the critical purpose of discriminating between healthy and unfit rails. In other words, the approach of setting a rigid threshold, or even a range of acceptable values, to determine the similarity of signals and hence health state of rail may not be the most effective. While the identification of similarities rests heavily on the pattern or shape of the decomposed signals, it is possible to make comparisons based on pattern recognition. As a large amount of signals on health rails are available from on-site measurement, a substantial database can be set up to support the training process of a pattern recognition mechanism, such as neural network.

Neural network enables pattern recognition while allowing for imprecision in the data [13, 14]. They work as memory which associates input patterns with corresponding output decision and the memory is trained by selected patterns. Neural network is robust and flexible enough to cater for variations or even exceptions in the signals. Thresholds and reference values are not required and the performance depends on the quality of training data and the network structure. Neural network is thus a promising tool for this application. The signal pattern recognition at each decomposed frequency band calls for an independent neural network and the overall decision is determined collectively by the outputs of all the neural networks.

The signal signature on a rail-wheel interaction may not be fully discovered yet because the decompositions through frequency bands with Wavelet Transform are limited by the number of

sample points available. Part of the signature may be buried in the lower frequency bands than this study reaches. When train speed increases, the signal duration is shorter and the number of sample points for the low frequency bands is even smaller. A simple solution is a higher sampling rate at each sensor.

The current sampling frequency of each FBG sensor is 1 kHz which is not particularly high for signal processing purposes. It is limited by the FBG interrogator which has to conduct sampling over the spectral width of 100 nm with one sensor occupying about 1 nm. The sampling rate of the interrogator is indeed very high (e.g. 100 kHz for 100 sensors sampling at 1 kHz) but sampling capacity allocated to each sensor is substantially reduced. FBG interrogators with higher sampling capability are available but they are very expensive. On the other hand, it is also possible to equip the interrogator with a light source of narrower spectra so that the interrogator is able to ‘focus’ on a smaller scope only but with higher sampling rate. The drawback is of course the reduced number of sensors being served and hence the whole setup is less cost-effective.

This study only examines the signals from healthy rails so far as they are the only available on-site measurement data. Signatures (or their changes) in the signals due to defects on rails or even different types of defects are useful to identify the key areas in the signal patterns for comparisons. However, for safety and reliability concerns, defective rails are often replaced as soon as they are located and data on rail-wheel interactions from unfit rails are not taken in practice. While such data cannot be reproduced in a laboratory, the closest resemblance of a real-life situation of rail-wheel interactions with known rail defects is under the controlled environment within a depot.

Defect detection is possible only if the change in the signal signature is picked up by the sensor. The magnitude (or other impacts) of the change in signal signature due to rail defect may have subsided and become undetectable if the distance between the defect and the sensor is excessive. Another important investigation is thus on the maximum distance between the defect and the sensor before the sensor fails to detect the defect. This effective sensing distance in turn determines the required number of sensors to be installed along the line, which is a critical consideration in the practical implementation of this endeavour of remote rail condition monitoring.

Conclusions

This paper presents a feasibility study on applying FBG sensors to detect rail defects through analysing the signals on rail-wheel interactions. Signal processing techniques have been adopted to extract the signatures and conduct comparisons. It has been established that the signal signatures on healthy rails are similar to a certain extent. However, the variations in the signals due to changes in operation conditions not related to the health state of the rails lead to difficulties in establishing clear-cut thresholds to single out defects. Detection through pattern recognition on signals in a number of decomposed frequency bands has then been suggested and discussed.

The main contribution of this study is the revelation of a number of practical difficulties and problems in measurement, equipment requirements and system setup. They are valuable for the further works in turning this promising application of advanced technologies into a new generation of remote rail condition monitoring system.

Acknowledgements

The authors would like to acknowledge the Hong Kong Polytechnic University for its generous support to this project. The authors also wish to express their gratitude to the MTR Corporation Limited for the permission on using the data collected from its railway line in this paper.

References

1. Clark, R., *Method and apparatus for testing rails for structure defects*, US Patent 5 970 438, (1999).
2. Marais, J.J., Mistry, K.C., Rail integrity management by means of ultrasonic testing, *Fatigue and Fracture of Engineering Materials and Structures*, vol. 26, no. 10, pp. 931-938, (2003).
3. Bhaskar, A., Johnson, K.L., Woodhouse, J., Wheel-rail dynamics with closely conformal contact part 1: dynamic modelling and stability analysis, *Proc. IMechE Part F*, vol. 211, pp. 11-26, (1997).
4. Bhaskar, A., Johnson, K.L., Woodhouse, J., Wheel-rail dynamics with closely conformal contact part 2: forced response, results and conclusions, *Proc. IMechE Part F*, vol. 211, pp. 27-40, (1997).
5. Lee, K.K., Ho, S.L., Unconventional method of train detection using fibre optic sensors, *HKIE Trans.* vol. 13, no. 1, pp. 16-21, (2006).

6. Guan, B.O., Tam, H.Y., Liu, S.Y. Temperature-independent fiber bragg grating tilt sensor, *IEEE Photonic Technology Letters*, vol.16, no.1, pp.224-226 (2004).
7. Chan, T.H.T., Yu, L., Tam, H.Y., Ni, Y.Q., Chung, W.H., Cheng, L.K., Fiber bragg grating sensors for structural health monitoring of Tsing Ma bridge: background and experimental observation, *Engineering Structures*, vol. 28, no. 5, pp. 648-659, (2006).
8. Ho, S.L., Tsang, W.F.S., Lee, K.Y., Lee, K.K., Lai, W.L.W., Tam, H.Y., Ho, T.K., Monitoring of the vertical sleepers with the passage of trains', *IET Intl. Conf. on Railway Condition Monitoring*, pp.108-114, (2006).
9. Lee, K.K., Ho, S.L., Lee, K.Y., Chan, H.K., Structural integrity of the body shells of light rail cars, *HKIE Trans.* vol. 13, no. 1, pp. 22-25, (2006).
10. Ho, T.K., Liu, S.Y., Ho, Y.T., Ho, K.H., Wong, K.K., Lee, K.Y., Tam, H.Y., Ho, S.L., Signature analysis on wheel-rail interaction for rail defect detection, *IET Intl. Conf. on Railway Condition Monitoring*, (2008).
11. Bentley, P.M., McDonnell, J.T.E., Wavelet transform: an introduction', *Electronics and Communication Engineering Journal*, pp. 175-186, (1994).
12. Schuler, C., Chugani, M., *Digital signal processing: A hand-on approach*, McGraw Hill, (2005).
13. Hagan, M.T., Demuth, H.B., Beale, M., *Neural network design*, PWS Publishing, (1996).
14. Bishop, C.M., *Neural networks for pattern recognition*, Oxford University Press, (1995).

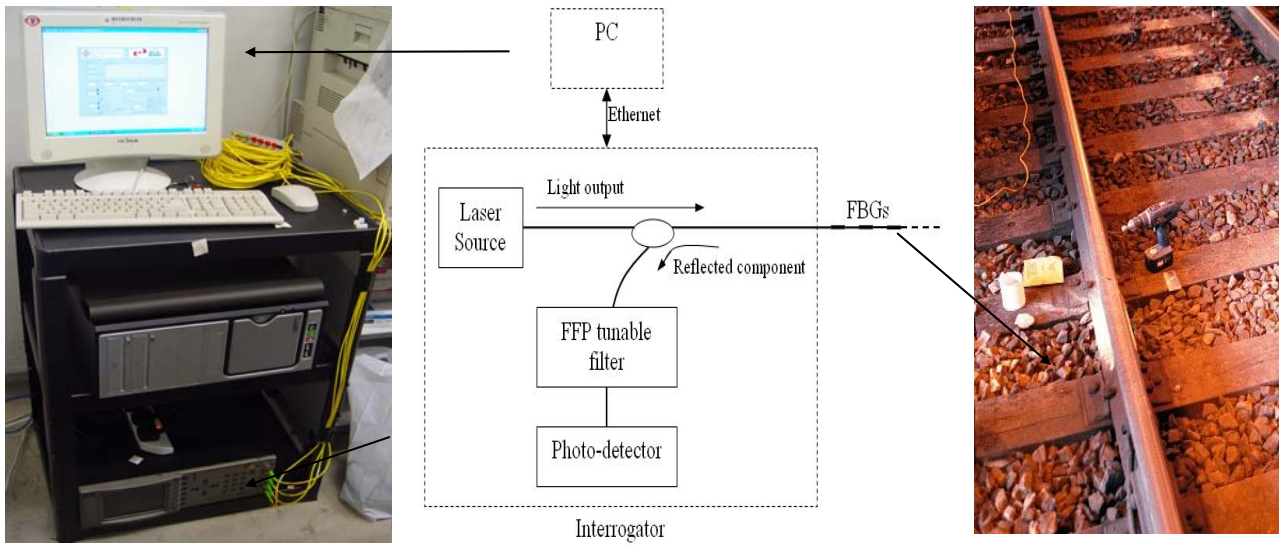


Figure 1: Optical fibre sensing system set-up

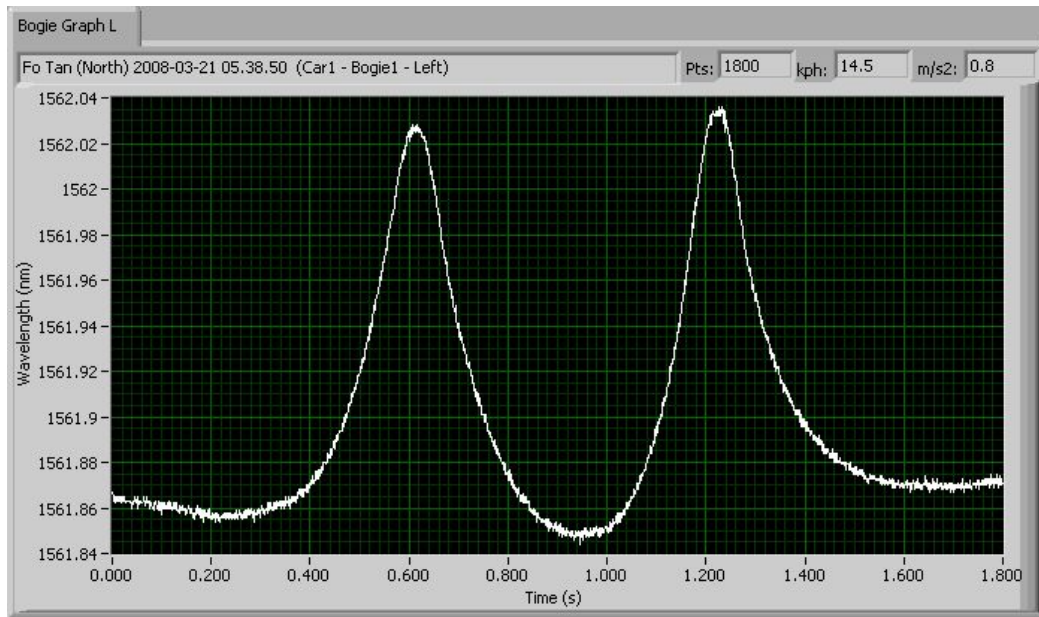


Figure 2: An example of data collected (for one bogie) from a FBG sensor near Fo Tan Station

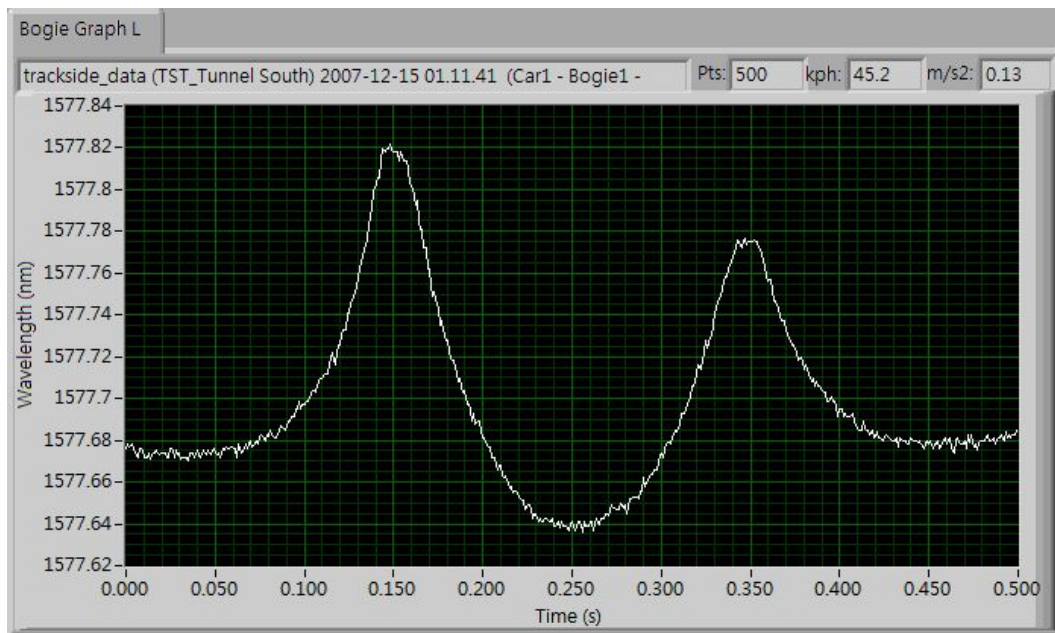


Figure 3: Data collected from a FBG sensor at TST Tunnel

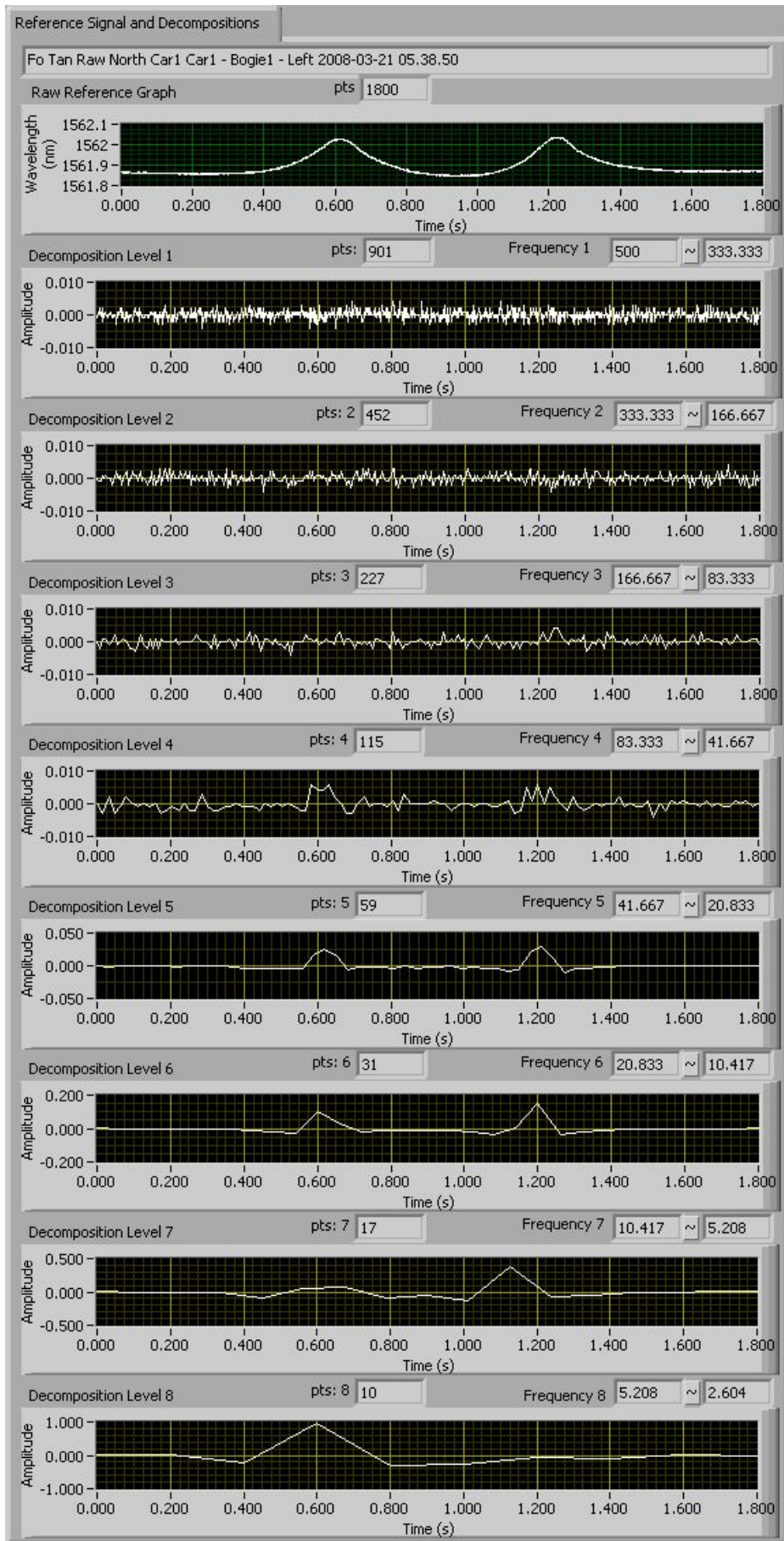


Figure 4: Decomposed signal upon Wavelet Transforms

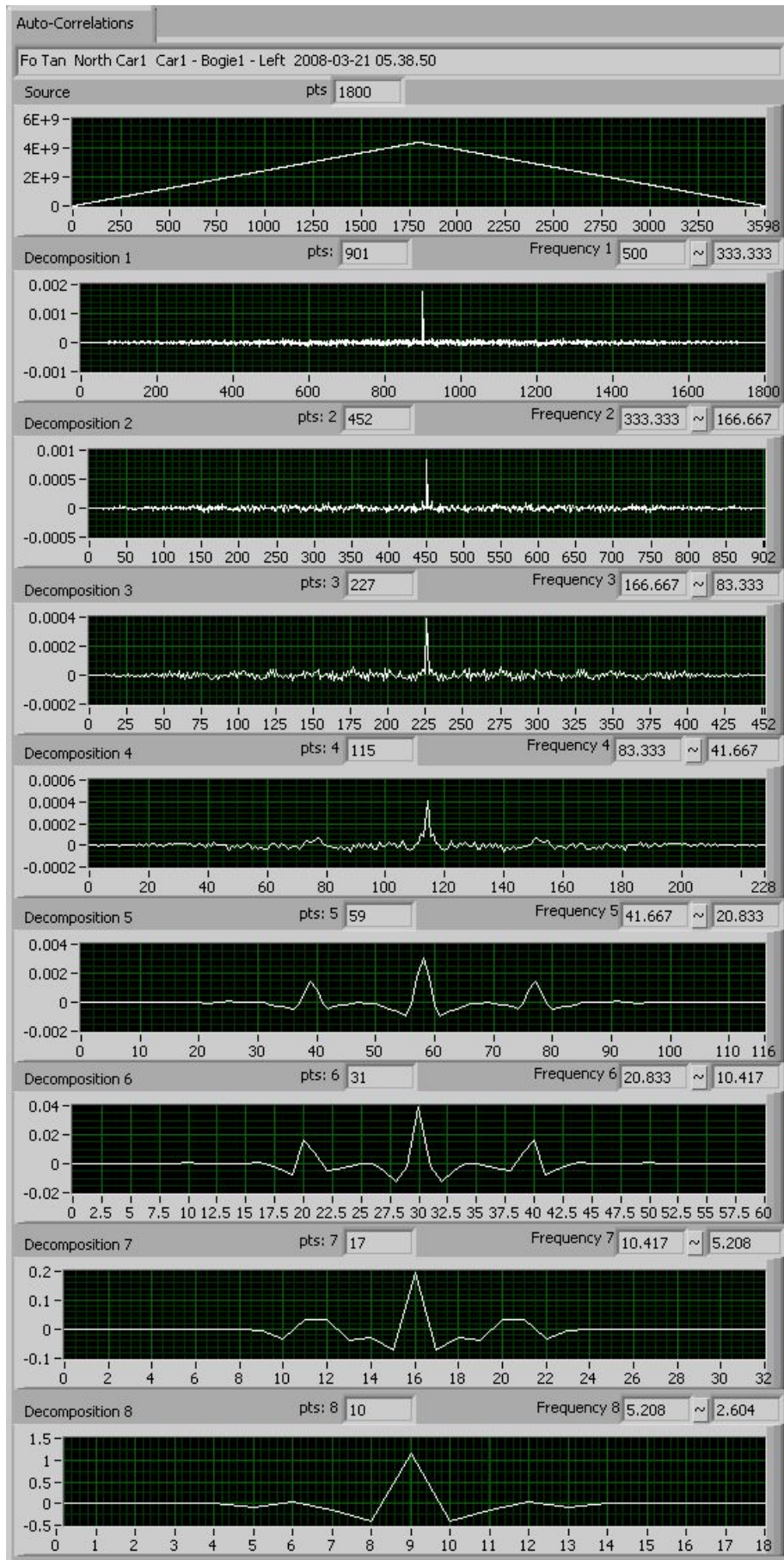


Figure 5: Auto-correlation on the decomposed signal at each frequency band

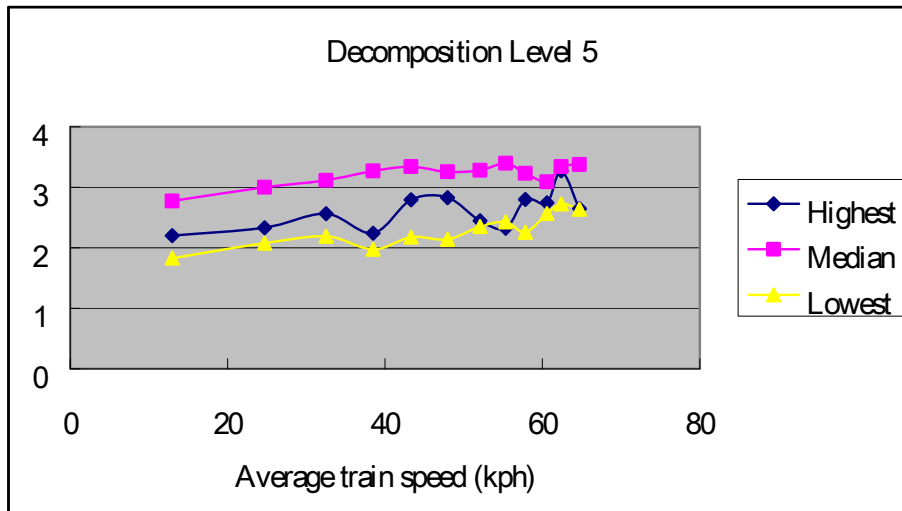


Figure 6: Average peak values of correlations on different train speeds (level 5 signals)

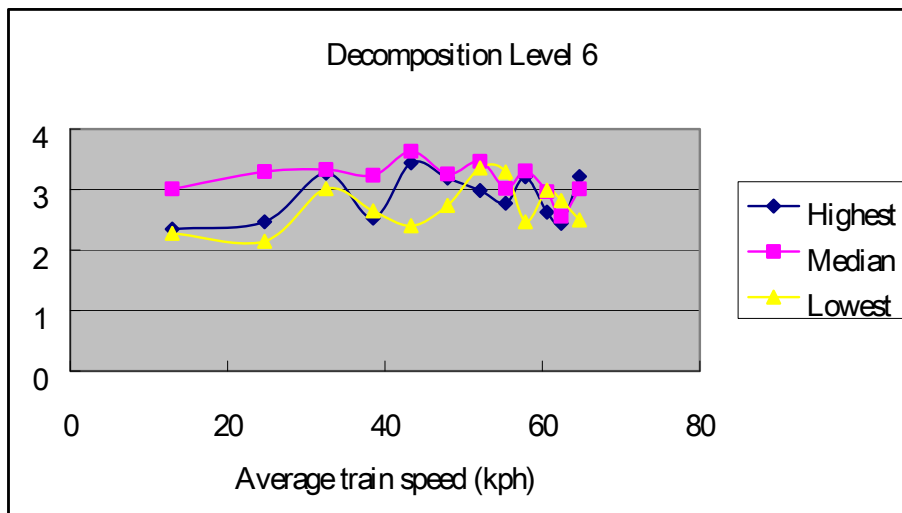


Figure 7: Average peak values of correlations on different train speeds (level 6 signals)

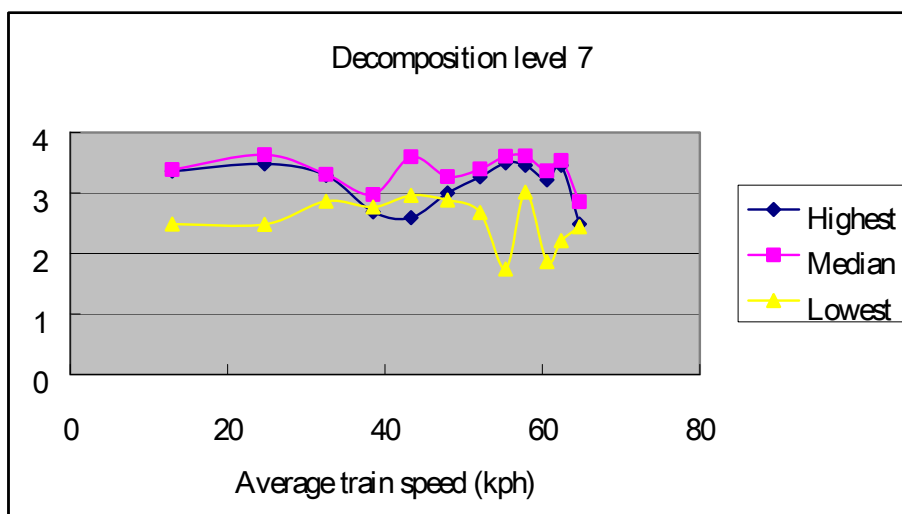


Figure 8: Average peak values of correlations on different train speeds (level 7 signals)

	Level 5 (41.67-20.83Hz)	Level 6 (20.83-10.42Hz)	Level 7 (10.42-5.21Hz)
Highest	6.345	3.781	4.357
Median	3.715	2.399	1.917
Lowest	1.787	1.512	1.271
Average	3.769	2.452	1.958
Standard Deviation	0.962	0.605	0.527

Table 1: Peak values of auto-correlation on signals at the decomposed frequency bands

References for cross-correlation		Level 5 (41.67-20.83Hz)	Level 6 (20.83-10.42Hz)	Level 7 (10.42-5.21Hz)
Highest speed 15.126 kph	Average	2.202	2.345	3.361
	Standard Deviation	0.588	0.580	0.456
Median speed 13.216 kph	Average	2.774	3.008	3.389
	Standard Deviation	0.667	0.703	0.570
Lowest speed 9.698 kph	Average	1.830	2.276	2.487
	Standard Deviation	0.417	0.466	0.589

Table 2: Peak values of cross-correlation on signals at the decomposed frequency bands